

KamLAND: Neutrinos from the Sun, the Earth and Nuclear Reactors

L. A. Winslow for the KamLAND Collaboration

*Massachusetts Institute of Technology, Laboratory for Nuclear Science, 32 Vassar St.
Cambridge, MA 02139, USA*



KamLAND is a one-kiloton liquid scintillating detector located in the Kamioka Mine in Kamioka, Japan. KamLAND measurements have shown evidence for neutrino oscillation in reactor anti-neutrinos and indications of geological produced anti-neutrinos. The first phase of KamLAND acquired almost 1500 days of data. An analysis of this full data set with improvements in calibration and the understanding of backgrounds now verify the spectral distortions predicted by neutrino oscillations at greater than 5σ . The fit to the data finds the neutrino oscillation parameters, $\Delta m_{21}^2 = 7.58_{-0.13}^{+0.14}(\text{stat.})_{-0.15}^{+0.15}(\text{syst.}) \times 10^{-5} \text{eV}^2$ and $\tan^2 \theta_{12} = 0.56_{-0.07}^{+0.10}(\text{stat.})_{-0.06}^{+0.10}(\text{syst.})$, the best determination of the mass difference for the foreseeable future. The details of this analysis is presented along with the current status and future plans for geo-neutrino and solar neutrino measurements with KamLAND.

1 Introduction

In the last decade, we have made great strides with our understanding of the physics of the neutrino. The results of the SNO experiment have shown that ^8B solar neutrinos change flavor as they propagate from the sun to the earth, thus solving the long standing Solar Neutrino Problem^{1, 2, 3}. The best explanation for this effect is that neutrinos have mass and therefore oscillate. The survival probability of electron flavored neutrinos or anti-neutrinos as a function of distance in vacuum is given by $P(\bar{\nu}_e \rightarrow \bar{\nu}_e) = 1 - \sin^2 2\theta_{12} \sin^2 \left(1.27 \Delta m_{21}^2 \frac{L(m)}{E(\text{MeV})} \right)$. KamLAND uses the nuclear reactors of Japan as a source of electron flavored anti-neutrinos and looks for the predicted deficit and spectral distortion at an average distance of 200 km^{4, 5, 6}.

The fissions in a nuclear reactor that are used to produce electricity also produce a significant number of $\bar{\nu}_e$, approximately 6 per fission. The fission isotopes that contribute significantly to the $\bar{\nu}_e$ flux are ^{235}U , ^{238}U , ^{239}Pu and ^{241}Pu . There are currently 55 nuclear reactors in Japan. The companies that operate these reactors provide us with the number fissions per isotope per day. A model of the reactor cores is then used to convert this information into a predicted flux and spectrum⁸. This modeling has an uncertainty of $\sim 2\%$. It has been suggested that this uncertainty is overestimated, and the systematic uncertainty due to the reactor prediction may be reduced⁷. On average 1 event per kiloton day is predicted at the KamLAND site. There have

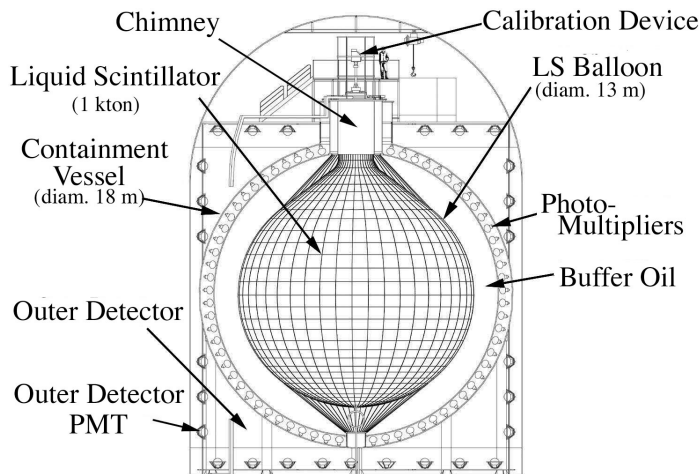


Figure 1: Diagram of the KamLAND detector. One kilo-ton of liquid scintillator(LS) is instrumented using photomultiplier tubes arranged on a stainless steel sphere.

been periods, that due to various issues with reactor operations in Japan, that this prediction has been as low as 0.5 events per kiloton day.

In addition to reactor anti-neutrinos, anti-neutrinos should also be produced by the natural decay of ^{238}U , ^{232}Th , and ^{40}K in the earth. These geologically produced anti-neutrinos, geo-neutrinos, are low in energy, have energies below 2.6 MeV and a predicted flux smaller than the reactor flux. Since the decays of ^{238}U , ^{232}Th , and ^{40}K produces a significant fraction of the Earth's heat, geo-neutrinos provide a novel tool for the study of the structure and dynamics of the Earth.

2 Detecting Anti-Neutrinos

KamLAND is a liquid scintillating detector located in the Kamioka mine at a depth of 2700 m.w.e.. As is shown in Figure 1, the detector consists of a stainless steel sphere instrumented with a total of 1879 photomultiplier tubes(PMTs). Of these PMTs, 1325 are Hamamatsu R7250 seventeen-inch PMTs and the remainder are Hamamatsu R3602 twenty-inch PMTs. Surrounding the sphere is a water Čerenkov anti-coincidence detector. The target volume, 1 kiloton of liquid scintillator(LS), is contained within a thin nylon balloon. The liquid scintillator is composed of 80.2% dodecane and 19.8% psuedocumene with 1.36 g/L of PPO (2,5-Diphenyloxazole). The psuedocumene produces scintillation light when charged particles move through it. The PPO shifts this light into wavelengths where the PMTs are more sensitive, and the dodecane increases the flashpoint of this mixture such that it conforms to the safety requirements of the mine.

Anti-Neutrinos are detected with the inverse beta decay interaction, $\bar{\nu}_e + p \rightarrow e^+ + n$, which has a threshold of 1.8 MeV. The positron annihilates immediately, depositing its kinetic energy and the energy of the annihilation gammas into the LS. The total energy of this event is related to the incoming anti-neutrino energy by $E = E_{\bar{\nu}} - 0.8 \text{ MeV}$ with an additional small recoil correction. The neutron takes $207.5 \pm 2.8 \mu\text{s}$ to thermalize and capture. More than 99% of the time, the neutron captures producing a 2.2 MeV gamma ray. These two events, the prompt positron annihilation and the delayed neutron capture, form a delayed coincidence signal which is extremely effective at reducing background contamination.

There are three main backgrounds that mimic the inverse beta decay signal: accidental coincidences, $^9\text{Li}/^8\text{He}$ spallation products, and $^{13}\text{C}(\alpha, n)^{16}\text{O}$ reactions. Accidental coincidences are the result of single events piling up within the coincidence time used to identify inverse beta decay events. This background becomes large as you move away from the center of the detector

Table 1: Estimated systematic uncertainties relevant for the neutrino oscillation parameters Δm_{21}^2 and θ_{12} .

| | Detector-related (%) | | Reactor-related (%) | |
|-------------------|----------------------|-----|-------------------------------------|-----|
| Δm_{21}^2 | Energy scale | 1.9 | $\bar{\nu}_e$ -spectra ⁹ | 0.6 |
| Event Rate | Fiducial volume | 1.8 | $\bar{\nu}_e$ -spectra | 2.4 |
| | Energy threshold | 1.5 | Reactor power | 2.1 |
| | Efficiency | 0.6 | Fuel composition | 1.0 |
| | Cross section | 0.2 | Long-lived nuclei | 0.3 |

due to the large amount of radioactive decays coming from the balloon surface. The isotopes ^9Li and ^8He are an issue because they are beta-delayed neutron emitters, the isotope beta decays to an excited state of the daughter nucleus that de-excites by emitting neutrons. These isotopes are created in muons spallation so their coincidence with muons can be used to eliminate them. The $^{13}\text{C}(\alpha, n)$ reaction occurs when a high energy alpha hits a ^{13}C nucleus making a neutron. This process can mimic an inverse beta decay signal in three ways. The neutron can be made with enough kinetic energy that the scattering of the neutron on protons creates enough light to trigger KamLAND. The neutron can excite a ^{12}C nucleus which de-excites with a 4.4 MeV gamma ray. The ^{16}O nucleus can be produced in an excited state that de-excites with a 6.05 MeV or 6.13 MeV gamma. In all three scenarios, the neutron then thermalizes and captures producing the delayed event.

Candidate inverse beta decay events are selected with cuts on the position and energy of the prompt and delayed events, and the time and distance between the events. The radial position of the prompt and delayed events (R_p, R_d) must be <6 m. The prompt energy is required to be between $0.9 \text{ MeV} < E_p < 8.5 \text{ MeV}$ where the lower bound is the inverse beta decay threshold and the upper bound is the endpoint of the reactor neutrino spectrum. The delayed event must have a reconstructed energy between $1.8 \text{ MeV} < E_d < 2.6 \text{ MeV}$ or $4.0 \text{ MeV} < E_d < 5.8 \text{ MeV}$ for capture on protons and ^{12}C , respectively. The coincidence requirement in time and space for the two events is $0.5 \mu\text{s} < \Delta T < 1000 \mu\text{s}$ and $\Delta R < 2$ m.

To reduce the number of $^9\text{Li}/^8\text{He}$ events in the sample, cuts are applied on the time and spatial separation of candidate event pairs and muons. Following muons that are well reconstructed, any candidate that occurs within 2 s and within 3 m cylinder around the track will be eliminated. Following poorly reconstructed muons or those that produce a large amount of light, all candidates within 2 s of the muon event anywhere in the detector are eliminated.

The radial position cut used in this analysis is larger than in previous analyses^{4,5}. A cut on a new variable L is constructed to mitigate the rise in the accidental background due to the proximity to the balloon. A probability distribution function (PDF) $f_{acc}(E_p, E_d, \Delta R, \Delta T, R_p, R_d)$ is constructed for the accidental background from the data in an off-time delayed coincidence window. A PDF for the anti-neutrino signal $f_{\bar{\nu}_e}(E_p, E_d, \Delta R, \Delta T, R_p, R_d)$ is constructed from a Monte Carlo using the measured neutron capture time and detector response. The variable L is then given by $L = f_{\bar{\nu}_e} / (f_{\bar{\nu}_e} + f_{acc})$ for each candidate pair. The value of the cut, L_{cut} is a function of the prompt event energy. In bins of 0.1 MeV, the value of L for which the number of events from the Monte Carlo $\bar{\nu}_e$ is greater than the number from the accidental event sample is used to set the L_{cut} in that bin for the anti-neutrino candidates.

3 Anti-Neutrino Analysis

The data for this analysis⁶ was acquired between March 9, 2002 and May 12, 2007. With the fiducial volume corresponding to $R < 6$ m, the exposure is 2.44×10^{32} proton-yr (2.881 kiloton-yr). The systematic uncertainty on fiducial volume in the past has been the largest systematic uncertainty^{4,5}. With the deployment of the Full Volume Calibration System¹⁰, we were able

Table 2: Estimated backgrounds after selection efficiencies.

| Background | Contribution |
|--|------------------|
| Accidentals | 80.5 ± 0.1 |
| ${}^9\text{Li}/{}^8\text{He}$ | 13.6 ± 1.0 |
| Fast neutron & Atmospheric ν | <9.0 |
| ${}^{13}\text{C}(\alpha, n){}^{16}\text{O}_{gs}$, np \rightarrow np | 157.2 ± 17.3 |
| ${}^{13}\text{C}(\alpha, n){}^{16}\text{O}_{gs}$, ${}^{12}\text{C}(n, n'){}^{12}\text{C}^*$ (4.4 MeV γ) | 6.1 ± 0.7 |
| ${}^{13}\text{C}(\alpha, n){}^{16}\text{O}$ 1 st exc. state (6.05 MeV e^+e^-) | 15.2 ± 3.5 |
| ${}^{13}\text{C}(\alpha, n){}^{16}\text{O}$ 2 nd exc. state (6.13 MeV γ) | 3.5 ± 0.2 |
| Total | 276.1 ± 23.5 |

to constrain the uncertainty in the reconstruction of events out to $R = 5.5\text{m}$ to $< 3\text{cm}$ using an array of radioactive sources. By studying the distribution of ${}^{12}\text{B}/{}^{12}\text{N}$ candidates in the scintillator, we are able to extrapolate the calibration points from the Full Volume Calibration System to $R < 6\text{m}$ and set the systematic uncertainty on the fiducial volume to 1.8%. The systematic uncertainties are summarized in Table 1. They are divided by their impact on the neutrino oscillation parameters Δm_{21}^2 versus θ_{12} . The dominant uncertainty on the event rate and, therefore, θ_{12} are reactor-related while the uncertainty in Δm_{21}^2 is dominated by our uncertainty on the conversion of reconstructed energy to real particle energy, the energy scale.

The prompt energy of the candidates extracted from the 2.44×10^{32} proton-yr data set using the analysis cuts summarized in the previous section are shown in Figure 2. There are 1609 candidates. The estimated background is 276.1 ± 23.5 events including the detection efficiency of each type of background is summarized in Table 2. The predicted number of reactor $\bar{\nu}_e$ without neutrino oscillation in this period is 2179 ± 89 events. The predicted number of geo-neutrino events is 56.6 or 13.1 including neutrino oscillation¹¹. This results in a deficit of $\bar{\nu}_e$ from neutrino oscillation with a significance of 8.5σ . The oscillation parameters are determined by an un-binned maximum likelihood fit that includes the energy and the reactor flux at the time of the event. This fit is shown in Figure 2. The best fit oscillation parameters are $\Delta m_{21}^2 = 7.58_{-0.13}^{+0.14}(\text{stat})_{-0.15}^{+0.15}(\text{syst}) \times 10^{-5} \text{eV}^2$ and $\tan^2 \theta_{12} = 0.56_{-0.07}^{+0.10}(\text{stat})_{-0.06}^{+0.10}(\text{syst})$ for $\tan^2 \theta_{12} < 1$. A simple scaling of the undistorted reactor spectrum, shown in black in Figure 2, is excluded at 5σ , making this a clear detection of spectral distortion due to neutrino oscillation. A nice visualization of the sinusoidal behavior of neutrino oscillation as a function of baseline divided by the event energy, L/E , is shown in Figure 3. The flux averaged baseline, $L_0 = 180\text{km}$, for this period is used to construct this plot.

The allowed contours for the neutrino oscillation parameters from the maximum likelihood fit are shown in Figure 4 including $\Delta\chi^2$ -profiles. Before the results of KamLAND^{4,5,6} and SNO^{1,2,3}, the parameter space for solar+reactor neutrino oscillation spanned several orders of magnitude in Δm_{21}^2 and $\tan^2 \theta_{12}$. Now, only a single island remains. Assuming CPT invariance, a two neutrino combined solar+reactor fit finds $\Delta m_{21}^2 = 7.59_{-0.21}^{+0.21} \times 10^{-5} \text{eV}^2$ and $\tan^2 \theta_{12} = 0.47_{-0.05}^{+0.06}$. It is interesting to note with the improved statistics and systematic uncertainties on the event rate, KamLAND is beginning to be as sensitive as the solar experiments to $\tan^2 \theta_{12}$. This slight tension between the solar and reactor measurements may be an indication of a non-zero value of θ_{13} ¹².

The rate of geo-neutrinos is included in the solar+reactor fit for the oscillation parameters. The ${}^{40}\text{K}$ geo-neutrinos are below the inverse beta decay threshold, so are not included in the fit. The ratio U/Th chain geo-neutrinos is fixed to 3.9, the value determined from chondritic meteorites¹³, to avoid a large anti-correlation between the fluxes from these two decay chains. The U+Th best-fit value is $(4.4 \pm 1.6) \times 10^6 \text{cm}^{-2}\text{s}^{-1}$ (73 ± 27 events), in agreement with the reference model¹¹, $4.14 \times 10^6 \text{cm}^{-2}\text{s}^{-1}$.

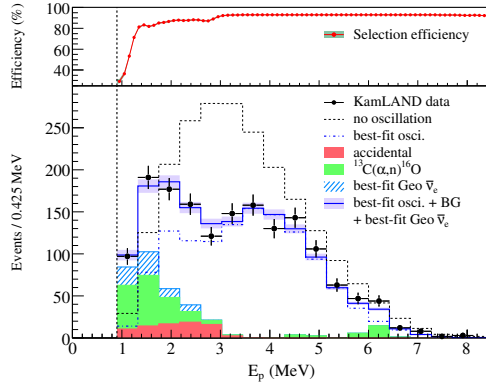


Figure 2: Prompt event energy spectrum of $\bar{\nu}_e$ candidate events. The statistical uncertainties is shown for the data points. The blue histogram only shows the event rate systematic uncertainty. The predicted histograms all include the energy-dependent selection efficiency shown in the top panel.

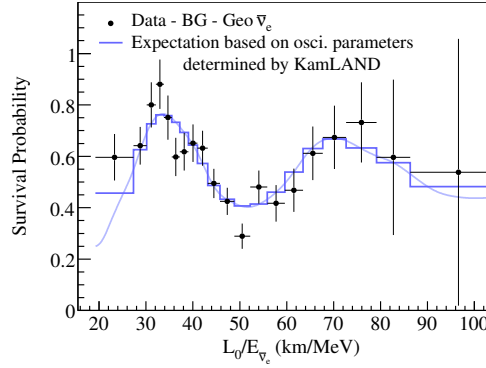


Figure 3: Ratio of the background and geo-neutrino-subtracted $\bar{\nu}_e$ spectrum to the expectation for no-oscillation as a function of L_0/E where L_0 is the flux averaged baseline taken as a of 180 km. The energy bins are equal probability bins of the best-fit including all backgrounds and the error bars are statistical only.

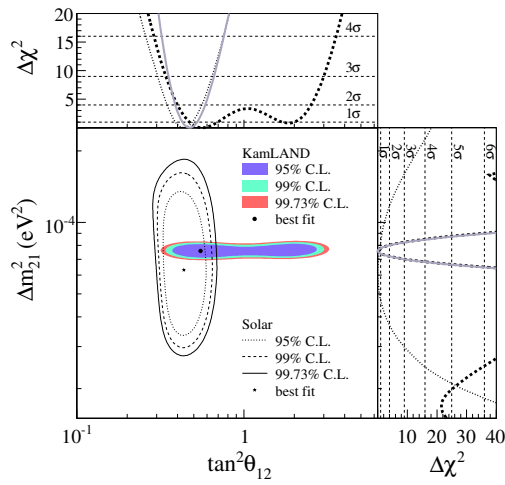


Figure 4: Allowed region for neutrino oscillation parameters from KamLAND and solar neutrino experiments. The side-panels show the $\Delta\chi^2$ -profiles for KamLAND (dashed) and solar experiments (dotted) individually, as well as the combination of the two (solid).

4 Future

KamLAND has definitively detected the spectral distortion predicted by neutrino oscillation in vacuum. The spectral distortion of solar neutrinos as they transition from matter to vacuum dominated oscillation still has not been observed. This is a small effect for the high energy ^8B neutrinos, those measured by SNO. The observation of this transition requires lower energy neutrinos, and the ^7Be neutrinos are ideally positioned to observe this effect. Unfortunately, the single event rate in KamLAND at these energies makes the observation of the elastic scatter of ^7Be neutrinos impossible. A purification system¹⁴ has been built to reduce the amount of ^{210}Pb and ^{85}Kr . A commissioning purification campaign took place in the Summer of 2007, followed by another campaign from the Spring of 2008 through the Winter of 2009. In this most recent campaign, 4.1 volumes of the KamLAND LS were exchanged, and the results are encouraging for a KamLAND observation of ^7Be neutrinos. A successful purification of KamLAND would also improve the reactor plus geo-neutrino analysis by eliminating the $^{13}\text{C}(\alpha,n)$ and reducing the accidental background.

Acknowledgments

The KamLAND experiment is supported by the Japanese Ministry of Education, Culture, Sports, Science and Technology, and under the United States Department of Energy Office grant DEFG03-00ER41138 and other DOE grants to individual institutions. The reactor data are provided by courtesy of the following electric associations in Japan: Hokkaido, Tohoku, Tokyo, Hokuriku, Chubu, Kansai, Chugoku, Shikoku and Kyushu Electric Power Companies, Japan Atomic Power Co. and Japan Nuclear Cycle Development Institute. The Kamioka Mining and Smelting Company has provided service for activities in the mine. The author was supported by the Nuclear Science Division of Lawrence Berkeley National Lab.

References

1. Q. R. Ahmad *et al.* [SNO Collaboration], Phys. Rev. Lett. **89** (2002) 011301
2. B. Aharmim *et al.* [SNO Collaboration], Phys. Rev. C **72**, 055502 (2005)
3. B. Aharmim *et al.* [SNO Collaboration], Phys. Rev. Lett. **101**, 111301 (2008)
4. K. Eguchi *et al.* [KamLAND Collaboration], Phys. Rev. Lett. **90**, 021802 (2003)
5. T. Araki *et al.* [KamLAND Collaboration], Phys. Rev. Lett. **94**, 081801 (2005)
6. S. Abe *et al.* [KamLAND Collaboration], Phys. Rev. Lett. **100**, 221803 (2008)
7. Z. Djurcic, *et al.*, J. Phys. G **36**, 045002 (2009)
8. K. Nakajima *et al.*, Nucl. Instrum. Meth. A **569**, 837 (2006)
9. B. Achkar *et al.*, Phys. Lett. B **374**, 243 (1996).
10. J. K. Busenitz *et al.* [KamLAND Collaboration], JINST **4**, P04017 (2009)
11. S. Enomoto *et al.*, Earth Planet. Sci. Lett. **258**, 147 (2007).
12. G. L. Fogli, E. Lisi, A. Marrone, A. Palazzo and A. M. Rotunno, arXiv:0905.3549 [hep-ph].
13. A. Rocholl and K. P. Jochum, Earth Planet. Sci. Lett. **117**, 265 (1993).
14. Y. Kishimoto [KamLAND Collaboration], J. Phys. Conf. Ser. **120**, 052010 (2008).